

Chapter 9

DIC Measurement of the Kinematics of a Friction Damper for Turbine Applications

L. Pesaresi, M. Stender, V. Ruffini, and C.W. Schwingshackl

Abstract High cycle fatigue (HCF) caused by large resonant stresses is a common cause for turbine blades failure. Passive damping systems, such as friction dampers are often used by aero-engine manufacturers to reduce the resonant stresses and mitigate the risk of HCF. The presence of friction dampers makes the dynamics of the system highly nonlinear, due to the complex stick-slip and separation phenomena taking place at the contact interface. Due to this nonlinear behaviour, an accurate understanding of the operating deflection shapes is needed for an accurate stress prediction.

In this study, digital image correlation (DIC) in combination with a high speed camera is used to provide insights into the kinematics of the damper in a recently developed test rig. The in-phase and out-of-phase first bending modes of the blades were investigated leading to a full field measurement of the global ODS of the blades, and the local motion of the damper against its platforms. A significant change in the blades operational deflection shape could be observed due to the damper, and the sliding and rolling motion of the damper during a vibration cycle was accurately visualised.

Keywords DIC measurement • Underplatform damper • Friction joint • Nonlinear dynamics • Stick-slip

9.1 Introduction

One of the most common causes of failure for turbine blades is high-cycle fatigue caused by large resonant stresses [1]. Passive damping systems, based on friction energy dissipation, are often used as an effective means to reduce these large resonant stresses. Various sources of friction dissipation were used in the past for turbine blades, with the most common relying on underplatform dampers [2]. The underplatform damper is a metal device which is located between the platforms of two adjacent blades, and it is loaded by the centrifugal force during operation. The presence of the damper shifts the resonance frequencies of the bladed disk upward, and also provides the energy dissipation to reduce the vibration amplitude of the blades [3, 4]. The dynamic behaviour of a bladed disk with a friction damper is strongly nonlinear due to the friction forces at the interfaces, and some difficulties arise to reliably predict the dynamic response. For this reason, simplified experimental set-ups are often used to reproduce the fundamental dynamics of the problem without the uncertainties of an engine test. One of the most common set-ups is a double blade configuration with a single damper between the two blades where the centrifugal load is simulated via loaded wires [3, 5–7]. The latest test rig of this kind, able to mimic the main dynamic characteristics of a real high-pressure turbine (HPT) blade, was developed at Imperial College London [8, 9] (see Fig. 9.1).

It is well known that the nonlinear dynamic response of bladed disk assemblies is highly dependent on the motion of the damper and its contact states (stick-slip-separation). In [7, 9] a laser set-up was used to track the motion of distinct points on the edge of the damper, giving a low resolution insight into the kinematics of the damper associated with the different vibration modes. In this study, a more advanced set-up based on a high speed camera together with digital image correlation (DIC) will be used to obtain a more complete and detailed picture of the kinematics of the blades and damper, as well as to identify the stick-slip and separation phases experienced at the contact interface.

L. Pesaresi (✉) • V. Ruffini

Department of Mechanical Engineering, Imperial College London, Exhibition road, SW72AZ, London, UK
e-mail: luca.pesaresi12@imperial.ac.uk

C.W. Schwingshackl
Imperial College London, Exhibition Road, SW7 2AZ, London, UK

M. Stender
Hamburg University of Technology, 21073, Hamburg, Germany

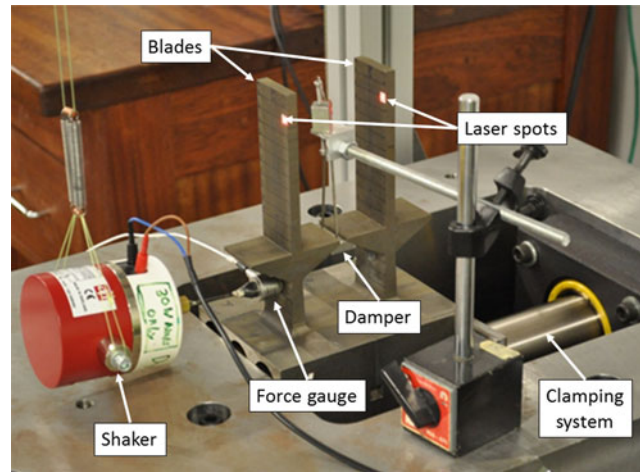


Fig. 9.1 UPD rig lab set-up

9.2 Underplatform Damper Test Rig

The underplatform damper (UPD) test rig is an experimental set up that allows the investigation of the effect of UPDs on blade like structures. A detailed discussion of the rig can be found in [9], and only a short discussion will be presented here for completeness. A static rig design was chosen to create a simplified experimental set up. The assembly of the rig can be seen in Fig. 9.1. Two pseudo beam-like blades are fixed to a common base, simulating a rigid disk, and are clamped via a hydraulic cylinder to a large inertia block. The damper is a wedge type, [3], which has a triangular cross section with a characteristic angle. Unlike a real high pressure turbine blade (HPT), the aerofoil is replaced by a straight rectangular cross-section beam, but still maintaining vibration modes similar to a real blade. The centrifugal load is simulated via a pulley system with calibrated masses, and the excitation is provided by an electrodynamic shaker attached near the root of the blade. Two single point laser Doppler vibrometers are used to measure the dynamic response of both blades at the tip.

9.3 Nonlinear Measurements

The nonlinear measurements focussed on the first flexural mode (1F), as it normally leads to the highest alternating stresses near the blade root. Two modes were investigated, the 1F out of phase mode of the blades (OOP) and the 1F in phase mode of the blades (IP). A stepped sine test was used for the excitation, where the level of shaker force was kept constant throughout the sweep. The excitation level was varied over a large range, from 0.01 N, where the response of the system was almost linear, to 17 N (shaker limit) where a strong nonlinearity was observed. The pulling load of the damper was kept constant at a high level (960 N) to ensure a good conformity at the contact interface. The evolution of the OOP and IP modes at various excitation levels can be observed in Fig. 9.2a, b.

The OOP mode (see Fig. 9.2a) shows a clear amplitude reduction, even present at lower excitation levels, and a slight frequency shift of about 2 Hz. This behaviour seems to indicate that the contact is experiencing “microslip”, as this slight frequency shift is normally caused by the progressive evolution of the contact interface from a fully stuck contact to a full slip condition. The IP mode, which was measured from high to low frequencies seems to be dominated by a significant FRF softening, characterised by the left-leaning and jumping response (see Fig. 9.2b). A possible explanation could be based on the tendency of the damper to roll in the IP mode [3, 7], which can reduce the damper-platform contact area at higher amplitudes, leading to a softer system. The dynamic behaviour of the IP and OOP modes varies quite strongly, and a good understanding of the blade and damper motion is needed.

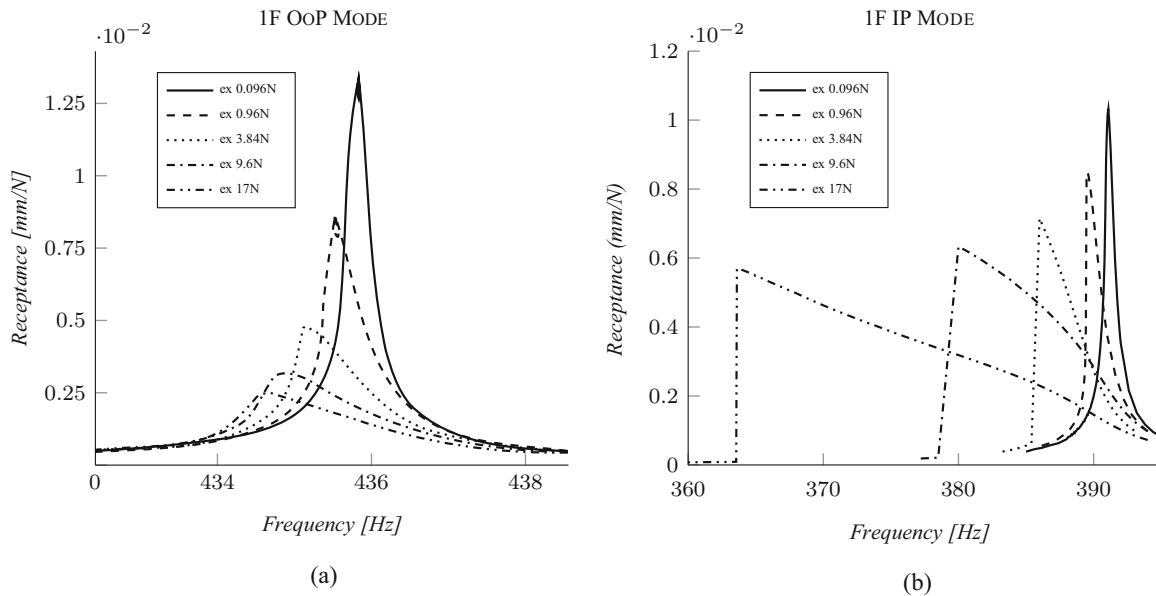


Fig. 9.2 Experimental FRFs at various excitation forces and constant damper load (960 N), (a) OOP mode, (b) IP mode

9.4 DIC Visualization of the UPD Test Rig

To investigate the motion of the damper and the blades during a nonlinear response of the system, a high speed camera set-up in combination with DIC analysis was used. The camera is a Photron Mini UX100 and is capable of 4000 fps at the full frame resolution (1280×1024 pixels). Two different Nikon lenses were used, a standard photographic Nikon DX SWM VR 18–55 mm to capture the whole blade and a Nikkor Micro SWM VR ED IF 105 mm lens which was used for a close up of the damper. The camera was aligned along an axis perpendicular to the lateral plane of the damper rig, as shown in Fig. 9.3, to allow a clear 2D view of the bending modes of the blades and the damper. Two LED spotlights were used to illuminate the structure and allow a higher camera shutter speed, thus avoiding the risk of blurred images.

Digital image correlation was used to analyse the recorded images and extract the displacement field for the damper and blades. DIC is a powerful tool as it allows the post-processing of the results of a contactless fullfield measurement system (high-speed camera) with a high spatial and temporal resolution. For this study, an open source Matlab-based code developed at the Georgia Institute of Technology, Ncorr, was used where the main components and concepts are described by Blaber et al. [10].

9.4.1 Operational Deflection Shape

The first application of the DIC was to investigate the change in the ODS caused by the presence of the damper. The presence of the damper stiffens the FRF of the blades significantly leading to a frequency shift from 269 to 392 Hz for the IP mode, and 435 Hz for the OOP mode. It is likely that such a fundamental change in frequency is associated with a different ODS which may lead to a different distribution of cyclic stresses, and therefore impact the expected life of the blades. The high-speed camera was adjusted to frame one of the two blades, and two spotlights directed towards the upper and lower part of the blade were used to have a uniform distribution of light (see Fig. 9.4).

After initial trials, a white and black random pattern was applied to the surface of the blade, as it significantly improves the signal to noise ratio of the DIC. The procedure used for the test was the following: (i) the frequency range of the mode of interest was identified, (ii) a stepped sine test was performed with a constant shaker excitation, (iii) at resonance a short video was recorded, and finally (iv) The DIC was then performed, and the average displacement for cross sections of the blade at increasing distances from the root was extracted. Three tests around the first bending mode were carried out, a low shaker level (0.5 N) test without the damper, a 17 N (shaker limit) test with the damper for the 1F IP and 1F OOP mode.

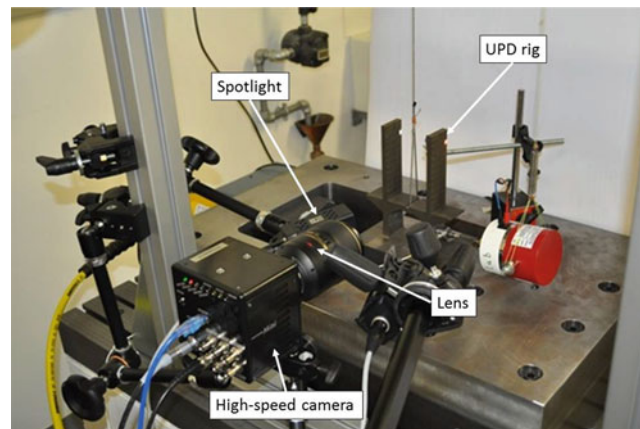


Fig. 9.3 High-speed camera set up applied to the UPD rig

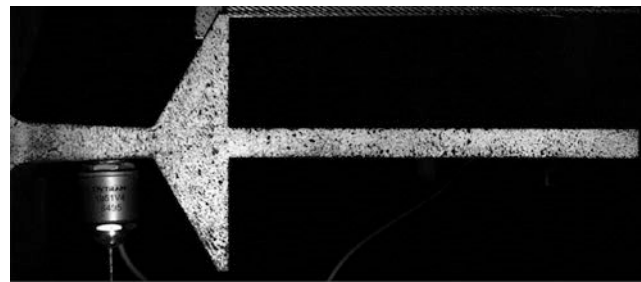


Fig. 9.4 High-speed camera view of the blade

When the damper was in place, the response level was much lower due to the added damping, leading to difficulties in the DIC post-processing at excitation amplitudes below 17N. The ODS results for the three tests and for different recorded frames are shown in Fig. 9.5. A change in shape for the 1F mode is evident when the damper is present, as the damper tends to couple the adjacent platforms and increases the curvature of the mode near the platforms. The IP mode is still very similar to the linear case without a damper but the OOP mode is very different (see Fig. 9.5d). The lower part of the blade is not deformed at all, and the blades tend to behave as a shorter beam. In this latter case, the peak stress is not expected near the blade root but higher up at the platform level, leading to a very different HCF scenario. These results show a great sensitivity of the DIC with regards to relatively small motions, since even the very small displacement close to the root (in the order of $10\ \mu\text{m}$) could be resolved. It should be said that the accuracy of the DIC may not be as accurate as that of an accelerometer or an LDV, but its relatively quick set-up and its provision of the full ODS in a single measurement clearly makes it a very interesting tool to investigate the nonlinear dynamic behaviour.

9.4.2 Damper Kinematics

The second application of the DIC was to investigate the kinematics of the damper associated with the different modes, to better understand the underlying nonlinear mechanism that drives the nonlinear response. The levels of displacement experienced by the damper are much lower than those of the blades, and for this reason the high-speed camera set-up was modified: a macro Nikkor lens was used to reduce the field of view to the damper, platforms and relative contact interface only (see Fig. 9.6a).

Once more a movie at 4000 fps and at full HD resolution was taken to capture the damper motion. A more detailed DIC analysis was then performed, with a grid of several tracking points in the region of the damper and the two platforms. A post-processing tool was developed in order to extract for each tracking point the absolute displacement against a reference image, which is then represented by a arrow. The displacement quiver plot obtained from the DIC analysis for the OOP and IP mode are shown in Fig. 9.7. The two frames shown for each mode are chosen near the maximum and minimum of the vibration amplitude. In the OOP mode (Fig. 9.7a, b), the damper has a pure vertical translation following the platform

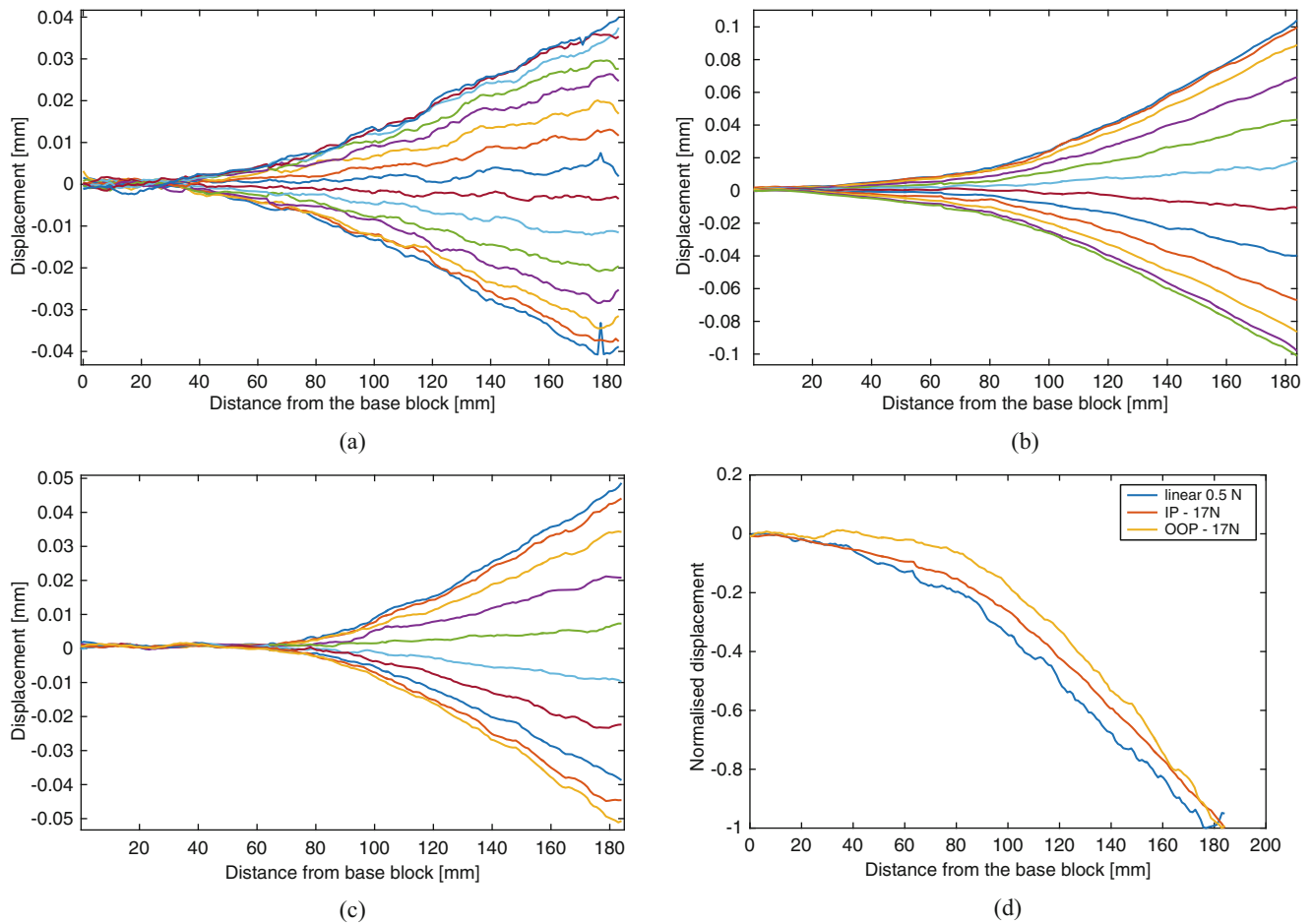


Fig. 9.5 DIC visualization of the blades ODS for different configurations: (a) linear without damper 0.5 N excitation, (b) with damper IP mode 17 N excitation, (c) with damper OOP mode 17 N excitation, (d) comparison of configurations normalised to relative max

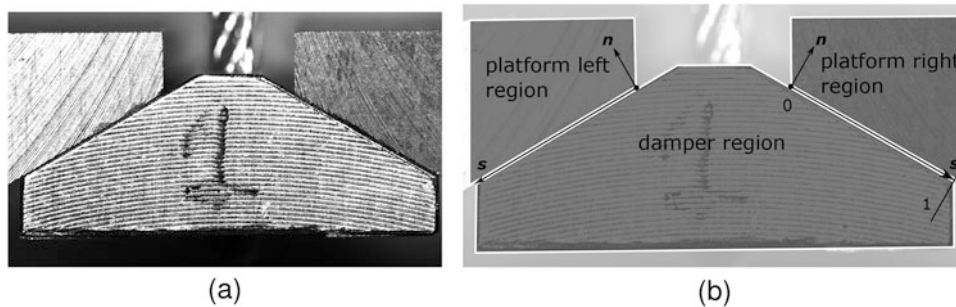


Fig. 9.6 (a) Camera view of the damper, (b) local coordinate system defined at the contact interface

motion. At the same time, the platforms tend to move to the sides, away from the centre of the frame when the damper is shifting up, and tend to move to the centre of the frame when the damper is shifting down. In Fig. 9.7c, d, which show the IP mode, the platforms exhibit an opposite vertical motion. As a consequence, following the platforms, the damper is subject to a counter clockwise rotation when the blades are moving to the right (Fig. 9.7c) leading to a horizontal translation. It is likely that this rotation leads to a change of the contact area at the interface, which can explain the strong softening of the FRF observed in the IP mode.

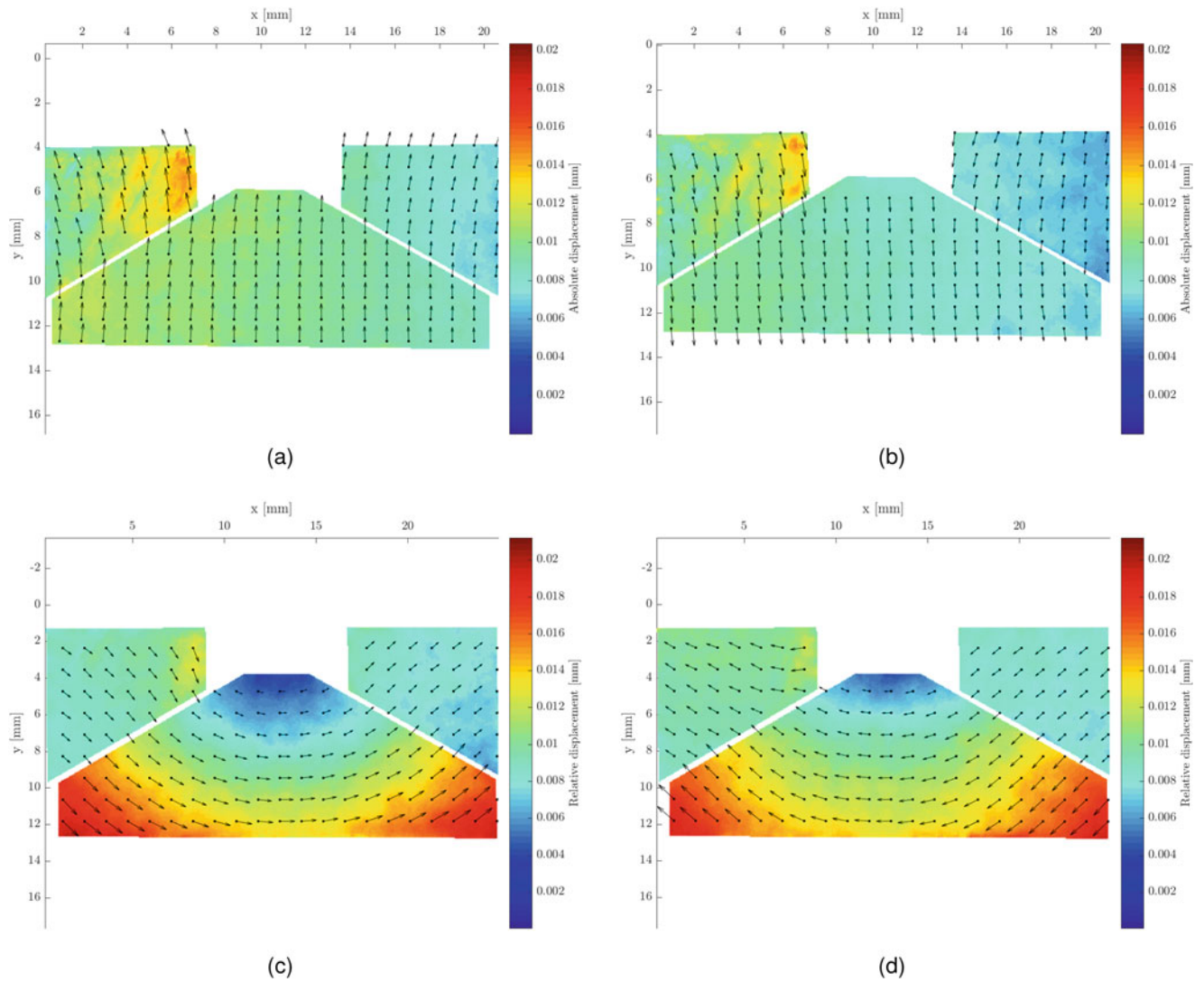


Fig. 9.7 DIC visualization of the kinematics of the damper: (a) first frame OOP mode, (b) second frame OOP mode, (c) first frame IP mode, (d) second frame IP mode

9.4.3 Damper Stick-Slip

To get a better understanding of the friction phenomena which are driving the nonlinear behaviour of the rig, a DIC analysis was performed at the contact interface. A post-processing tool was developed to calculate the relative contact motion at the interface, and evaluate the potential areas of slip, microslip or separation. A contact line was defined for the right and left interface (see Fig. 9.6b), and the tracking points in the vicinity of the contact line were divided into two groups, depending on whether they belonged to the damper or the platform. A local coordinate system was then defined in order to decompose the local displacement into normal and tangential components at the interface. To analyse the relative damper-platform displacement, it was necessary to unload the damper to 120 N since it was not possible to have a good signal to noise ratio with the 960 N preload used earlier, even at the highest excitation level (17 N).

Figures 9.8 and 9.9 show subsequent frames of the normal (\perp) and tangential (\parallel) displacement for both damper and platform, allowing a direct comparison between the two in order to detect stick-slip and separation phases. In particular, when the two lines are not overlapped, a separation is expected for the normal displacement plots, and a slip phase is expected for the tangential displacement plots. Looking at the OOP mode (see Fig. 9.8), it seems that the platform-damper interface is always in contact even if a slight separation could be observed in Fig. 9.8e, f near the bottom edge. In this mode a strong energy dissipation is expected, looking at the large macroslip observed in Fig. 9.8c–e where the damper is slipping

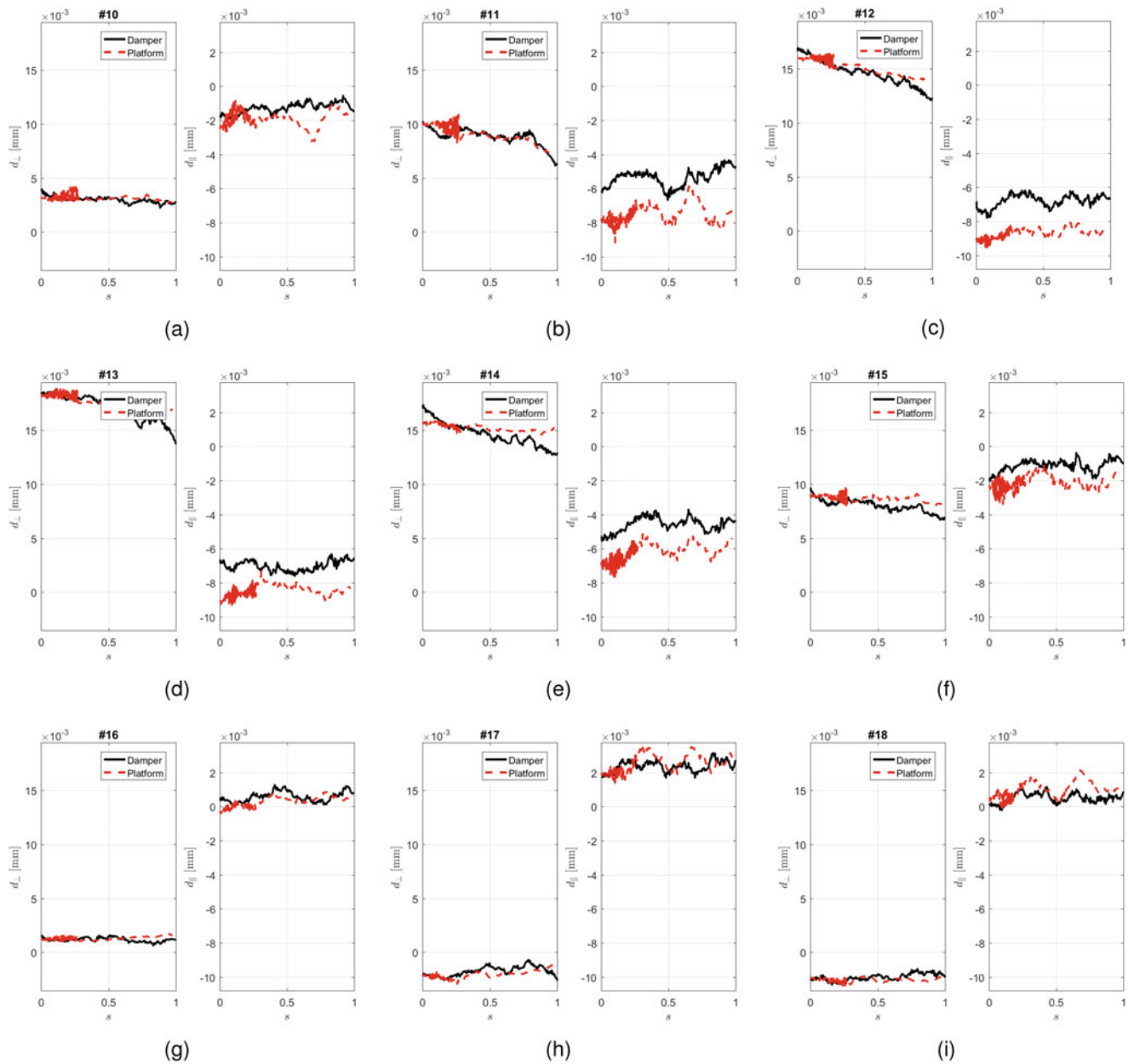


Fig. 9.8 DIC visualization of subsequent frames of the right contact displacement for both damper and platform, OOP mode

and in contact at the same time. This strong energy dissipation was supported by the nonlinear measurements in Fig. 9.2a where a higher damper load was used there. With regards to the IP mode (Fig. 9.9), a partial loss of contact can be observed for most of the frames captured indicated by the difference in displacement in the normal direction. In particular, Fig. 9.9h, i show that only a small part close to the upper edge is in contact, whereas the lower part experiences a separation of more than 10 microns. This strong separation explains the softening of the FRFs observed in the blades response at high excitation levels (see Fig. 9.2b). Only a small tangential relative displacement is visible in Fig. 9.9b, d, h which is much less dominant than for the OOP mode. This small tangential displacement ties up with the nonlinear measurements (see Fig. 9.2b), where high excitation levels did not lead to significant amplitude reduction in the response of the IP mode.

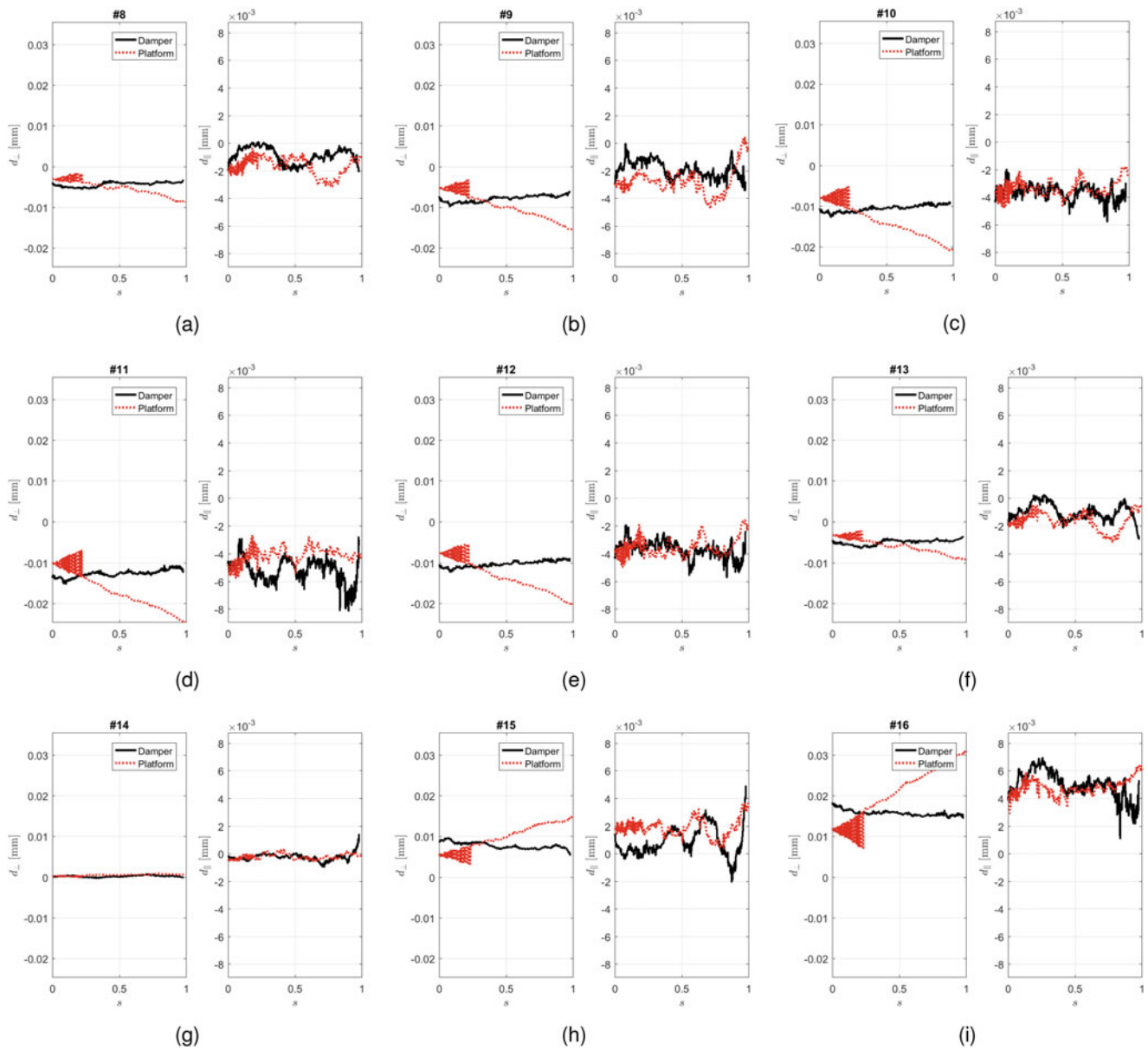


Fig. 9.9 DIC visualization of subsequent frames of the left contact displacement for both damper and platform, IP mode

9.5 Conclusions

In this study, a high-speed camera set-up in combination with a DIC analysis was applied to a recently developed underplatform damper test rig to obtain a more detailed understanding of the global and local motion of the system. The nonlinear response for the first flexural in-phase (IP) and out-of-phase (OOP) mode were measured, highlighting that at high amplitudes there was significant energy dissipation for the OOP mode and a strong softening with jumps for the IP mode.

An initial DIC analysis was focused on measuring the ODS of the two blades to gain an understanding of the change in the blade motion caused by the presence of the damper. The IP mode only showed a small change in the ODS, but the OOP was significantly altered with much less motion close to the root, and a strong curvature near the damper location, indicating a strong restraint from the damper.

Focusing the DIC analysis on the damper itself highlighted a pure damper translation for the OOP mode and a rotation for the IP mode. Zooming in even further on the contact interface, and tracking its motion during a vibration cycle, it was

possible to identify the different phases of stick-slip and separation which occurred in the μm range. The most evident aspects observed were a strong separation for large part of the contact area in the IP mode, and macroslip in the OOP mode.

The high speed camera in combination with DIC post-processing proved to be a powerful tool to understand more closely the local mechanisms which are responsible for the nonlinear dynamics of turbine blades constrained by friction dampers. Therefore, DIC methods offer great opportunities for the validation of numerical simulation results as complete displacement fields can be obtained, and are a welcome extension in the tool set to investigate the nonlinear behaviour of joints.

Acknowledgements The authors are grateful to Innovate UK and Rolls-Royce plc for providing the financial support for this work and for giving permission to publish it. This work is part of a collaborative R&T project SILOET II P19.6 which is co-funded by Innovate UK and Rolls-Royce plc and carried out by Rolls-Royce plc and the Vibration UTC at Imperial College London.

References

1. Cowles, B.A.: High cycle fatigue in aircraft gas turbine – an industry prospective. *Int. J. Fract.* **80**, 147–163 (1996)
2. Griffin, J.H.: A review of friction damping of turbine blade vibration. *Int. J. Turbo Jet Engines* **7**, 297–307 (1990)
3. Sanliturk, K.Y., Ewins, D.J., Stanbridge, A.B.: Underplatform dampers for turbine blades: theoretical modeling, analysis, and comparison with experimental data. *J. Eng. Gas Turbines Power* **123**(4), 919 (2001)
4. Sanliturk, K.Y., Ewins, D.J., Elliott, R., Green, J.S.: Friction damper optimization: simulation of rainbow tests. *J. Eng. Gas Turbines Power* **123**(4), 930 (2001)
5. Panning, L., Sextro, W., Popp, K.: Optimization of interblade friction damper design. In: *Proceedings of ASME TURBOEXPO*, pp. 1–8 (2000)
6. Pfeiffer, F., Hajek, M.: Stick-slip motion of turbine blade dampers. *Philos. Trans. R. Soc. Lond. A* **338**, 503–517 (1992)
7. Firrone, C.M.: Measurement of the kinematics of two underplatform dampers with different geometry and comparison with numerical simulation. *J. Sound Vib.* **323**(1–2), 313–333 (2009)
8. Pesaresi, L., Salles, L., Elliot, R., Jones, A., Green, J.S., Schwingshackl, C.W.: Numerical and experimental investigation of an underplatform damper test rig. *Appl. Mech. Mater.* **849**(1–12), 10 (2016)
9. Pesaresi, L., Salles, L., Jones, A., Green, J., Schwingshackl, C.: Modelling the nonlinear behaviour of an underplatform damper test rig for turbine applications. *Mech. Syst. Signal Process.* **85**, 662–679 (2017)
10. Blaber, J., Adair, B., Antoniou, A.: Ncorr: open-source 2D digital image correlation Matlab software. *Exp. Mech.* **55**(6), 1105–1122 (2015)